ACS OMEGA

Article

Cite This: ACS Omega 2018, 3, 2396−2405

Combined Adsorption and Covalent Linking of Paclitaxel on Functionalized Nano-Graphene Oxide for Inhibiting Cancer Cells

Wei Zhuang,*[,†,‡,∥] Linjiao He,[‡] Kai Wang,[⊥] Bo Ma,[§] Lei Ge,[#] Zhenfu Wang,[‡] Jinsha Huang,[‡] Jinglan Wu,[‡] Qi Zhang,[§] and Hanjie Ying[†,‡]

[†]State Key Laboratory of Materials-Oriented Chemical Engineering, Nanjing Tech University, No. 5 Xinmofan Road, Nanjing 210009, China

[‡]National Engineering Technique Research Center for Biotechnology, College of Biotechnology and Pharmaceutical Engineering and [§]School of Pharmaceutical Science, Nanjing Tech University, No. 30 Puzhu South Road, Nanjing 211816, China

[∥]School of Chemical Engineering, The University of Queensland, St Lucia, Queensland 4072, Australia

[⊥]Freshwater Fisheries Research Institute of Jiangsu Province, No. 79 Chating East Street, Nanjing 210017, China

[#]Centre for Future Materials, University of Southern Queensland, Springfield, Queensland 4300, Australia

ABSTRACT: Developing targeted delivery nanosystems for delivering chemotherapeutic anticancer drugs specifically to cancerous tissues with improvement in the specificity of drugs for different cancer cells can result in high therapeutic efficacy and low toxicity in healthy tissues. Herein, we proposed the synthesis of a multifunctional nanodelivery system, folic acid (FA) decorating nanographene oxide (nGO) functionalized with poly-(ethylene glycol) (PEG), called pGO-FA, with good biocompatibility and good delivering performance of a hydrophobic water-insoluble anticancer drug of paclitaxel (PTX). 4-br-PEG-NH_2, FA, and PTX were attached to PEG-functionalized nGO (pGO) through a combined chemical and physical force to form a nanosized complex, pGO-FA-PTX, defined as the nanodrug system. WST-8 assay in vitro illustrated that pGO-FA-PTX inhibited A2780 cells in a concentration-dependent manner. Cell viability was kept high to 60% when treated with 200 nM of free PTX. However, pGO-FA-PTX with the same dose of PTX (cell viability less than 30%) had double the cytotoxicity effect compared to free PTX. Furthermore, fluorescence observation demonstrated that pGO-FA-PTX exhibited an improved efficiency in killing A2780 cells due to the special affinity between FA and FA receptor, which has high expression in cancer cells. The strategy and method used in this study could be effective in improving both the bioavailability of PTX and therapy efficiency.

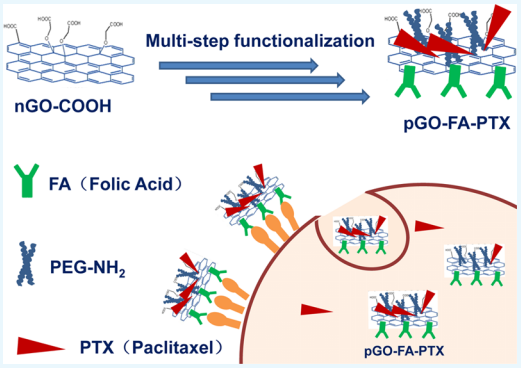

INTRODUCTION

Cancer is one kind of disease that results in several millions of deaths every year.[1] Chemotherapy plays a vital role among current treatment methods.[2] However, free drug chemotherapy has several limitations, such as nonspecific selectivity to cancerous tissues, poor water solubility of drugs, low local therapeutic concentration, and side effects to normal healthy cells.[3,4] To tackle these limitations, nanodelivery systems (NDS's)[1] including polymer nanoparticles,[5] mesoporous silica nanoparticles,[6] liposomes,[7] microspheres,[8] and inorganic materials[9] have been developed as anticancer drug carriers. On the account of these NDS, drugs can be directly conveyed into targeted cancer cells by connecting with target molecules and released under controlled conditions.[10] Nevertheless, the therapeutic efficiency of NDS is still unsatisfied owing to the low loading capacity and loading efficiency.[11] These challenges have driven the further development of drug delivery complexes.[1,12]

Paclitaxel (PTX) is a commonly used potent chemotherapy drug that shows high cytotoxicity to cancer cells.[3,12,13] PTX was considered as the most significant progress in tumor chemotherapy in recent decades by the National Cancer Institute (NCI) since its extraction from *Taxus brevifolia*.[14,15] However, the poor water solubility and poor bioavailability limited the clinical application of PTX.[14]

Graphene oxide (GO), a kind of famous two-dimensional (2D) advanced material, exhibited some remarkable biological and physical properties, such as excellent biocompatibility and solubility, super-structural stability, high drug loading amount, and controlled drug release behavior.[16−19] These advantages allowed GO to be a biological vector for medical imaging and drug delivery.[20] The existence of oxygen-rich groups such as carboxyl, hydroxyl, and epoxy groups at the surface enabled the stable GO suspension in pure water. However, GO will aggregate in ionic solutions that are rich in different kinds of salts or peptides and proteins, such as the normal cell medium

Received: December 19, 2017
Accepted: February 12, 2018
Published: February 27, 2018

DOI: 10.1021/acsomega.7b02022
ACS Omega 2018, 3, 2396−2405

and serum.[20] Furthermore, cytotoxicity tests have shown that GO exhibited a certain toxicity to cells and tissues, whereas well-functionalized GO with surface coated by polymers with biocompatibility was not obviously toxic at the tested doses.[21,22] Therefore, the modification of GO through covalent or noncovalent functionalization, specifically, covalent grafting of polymers onto GO sheets, can be a promising step for biomedical applications.[16,23,24]

Poly(ethylene glycol) (PEG) is an efficient polymer in biology due to its biocompatibility, slightest toxicity, protein resistance, and good solubility in water or other common solvents.[11,15,25,26] The combination of PEG with other polymers or nanoparticles can effectively improve their biocompatibility.[25,27,28] The surface modification of nanoparticles with PEG has been widely employed in drug delivery systems.[11,14] Moreover, for amino-functionalized linear polymer molecules of PEG-NH_2, fraction of alkyl chain connect to the surface, the other section available to the interior decorating, and then long PEG brushes can be formed on the carriers. Also, PEG-NH_2 is a very important surface functional material with many advantages, such as good hydrophilic properties, biocompatibility, and low costs, very similar to PEG.[29]

Therefore, PEGylation of graphene oxide can act as a desired carrier for delivering hydrophobic anticancer drugs. In a previous report, Liu et al., for the first time, synthesized and functionalized nanographene oxide (nGO) sheets with PEG-NH_2 to improve the aqueous solubility and dispersion stability of nGO in some physiological solutions. This functionalization also keeps the unique ability of nGO in the loading and delivery of aromatic, water-insoluble drugs, a camptothecin analogue (SN38), by physisorption.[20] After that, Xu et al. reported the chemically and physically loaded PTX onto the GO-PEG nanocarrier to afford a nanosized complex, GO-PEG/PTX and GO-PEG-PTX.[14] These studies explored the potential application of GO-PEG in biomedicine.[3,17]

The creation of specific target and the elimination or illumination of damaged cancer tissues require careful controlling of the shape, size, surface coating, and surface functionality of the NDS.[1,30,31] It is important to design the experimental parameters that must be helpful to produce nanodelivery systems that can keep its function but overcome the biological barriers.[32,33] Thus, targeting moieties or ligands should be chosen based on their physical properties against tumor cell specific receptors, their binding properties onto the particulate carriers, and their remaining functionally activities.[6] Among them, folic acid (FA), as a target molecule, was extensively applied in target cancer treatments study.[10,34−36] The folate receptor (FR) with a high selective affinity for FA can be overexpressed on the outside cell membrane of many cancer tissues.[36] In doing so, the attachment of FA and PEG-NH_2 onto the surface of GO can improve the transportation performance of nanocomplex into the FR-positive cancer cells through reasonable targeting.

Physical adsorption and chemical bonding of cancer therapy drugs to nanodelivery carriers involving drugs on the internal or external surfaces are described during the formation of different functionalities.[8,37,38] In this paper, we proposed new GO-based drug delivery systems, as shown in Scheme 1, for cancer therapy with improved utilization rate of PTX.

The nanocarrier of GO was prepared first by a modified Hummer's method and then surface grafted by biocompatible 4-armed starlike PEG-NH_2 to render the aqueous stability and biocompatibility (called pGO). Next, folic acid (FA) was

Scheme 1. Procedure of the Preparation of pGO-FA-PTX Nanodrug Delivery Systems

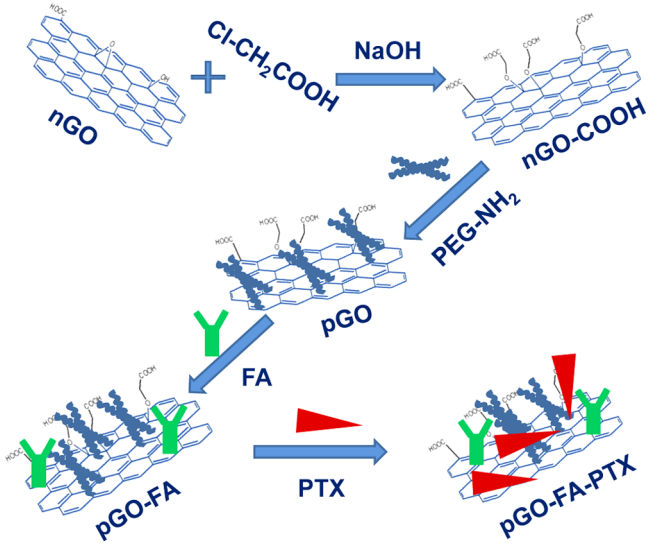

chemically reacted with pGO through amidation, successfully introducing a target recognition (called pGO-FA). Finally, PTX was physically and chemically loaded onto the pGO-FA nanocarrier to form a nanosized complex, pGO-FA-PTX. The successful functionalization of GO was verified by atomic force microscopy (AFM), Fourier transform infrared (FT-IR) spectrum, Raman spectroscopy, and ultraviolet and visible spectrophotometry (UV−vis).

Ovarian cancer is the most deadly cancer because of lack of early detection and effective therapy methods for late stage.[39] Evaluating the tumor models of A2780 cell line of human ovarian cancer tissue from an untreated patient is an important part of the drug discovery.[40] The derived nanocomplex could be efficiently taken up by cell line A2780 from the intracellular imaging. There is evidence that platinum-based chemodrugs and PTX can be given safely for cancer patients. But PTX is commercially available and active.[41] It was found from cell viability assay that pGO-FA-PTX could be an effective potential killer of cancer cells with a higher cytotoxicity to A2780 cells in vitro compared to free PTX. This proposed method could significantly improve the bioavailability of PTX and other hydrophobic drugs. The complex forces between the drug and carrier can give extend effective duration via controlled slow release.

RESULTS AND DISCUSSION

Water-soluble drug carrier of nGO was produced by a modified Hummer's method followed by high-power sonication.[18,42] The morphology of GO before surface modification was revealed by field emission scanning electron microscopy (FESEM) studies.[45] As shown in Figure 1a,b, dried nGO sheets stacked onto each other and formed thicker sheets owing to the interlayer $\pi-\pi$ interactions. It exhibited hundreds of nanometers lateral size and layered structure. Additionally, the morphology of nGO were also observed by transmission electron microscopy (TEM), as shown in Figure 1c,d, which showed a smooth and naked nGO surface with many silk-like wrinkles, and the lateral size is around 100 nm, which is very similar to that of the nGO used to penetrate into the cells.[46]

To further characterize the 2D and three-dimensional (3D) surface morphologies, as well as the thickness of the nGO,

DOI: 10.1021/acsomega.7b02022
ACS Omega 2018, 3, 2396−2405

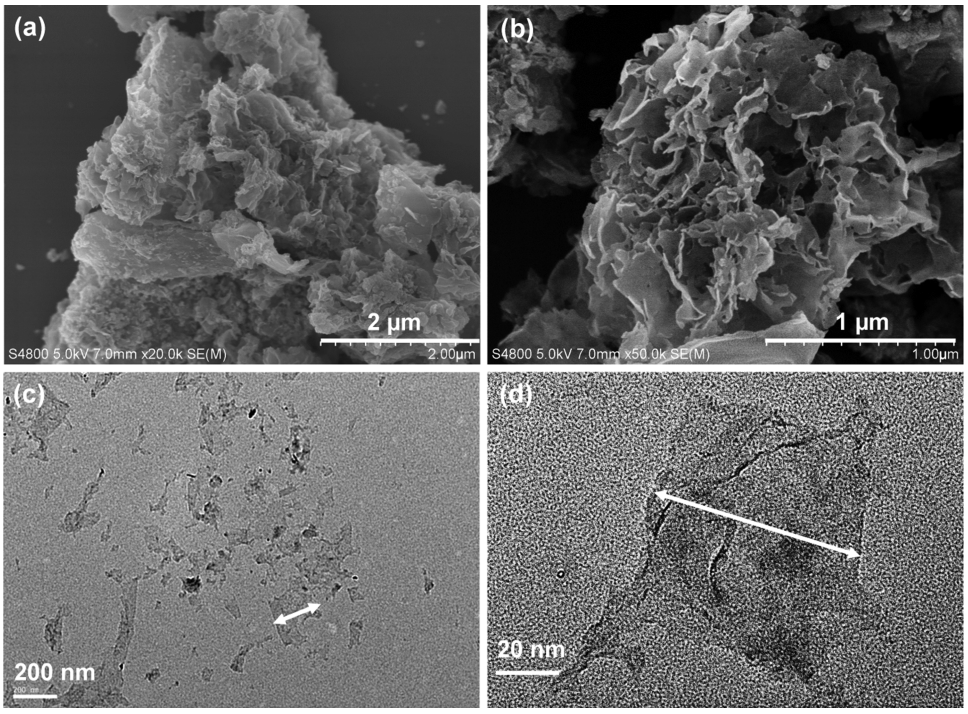

Figure 1. Morphology characterization of the nanodrug carriers of nGO: (a, b) FESEM images of nGO and (c, d) TEM images of nGO (the arrows help recognizing the edges of the nGO sheets).

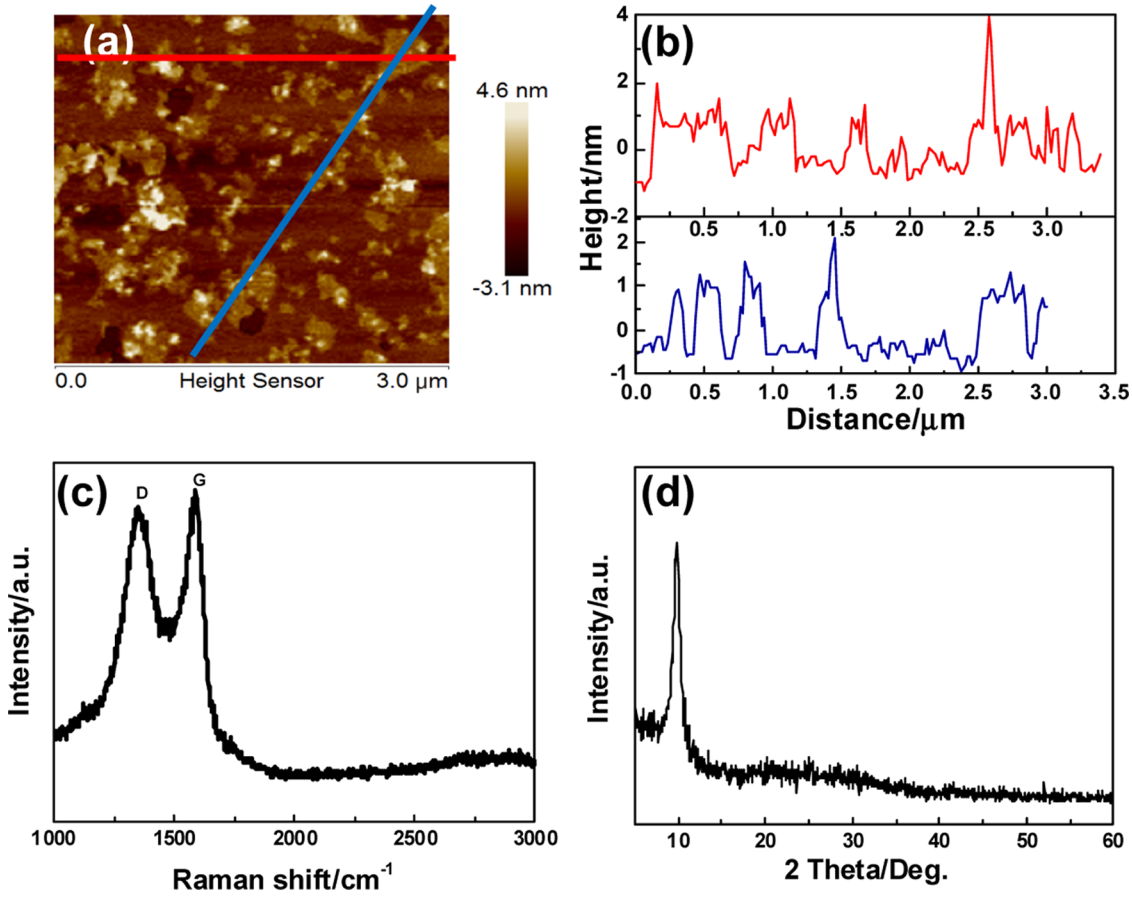

Figure 2. Structural characterization of nGO nanosheets: (a) AFM image of the as-synthesized nGO nanosheets; (b) height profiles of line scannings; (c) Raman spectrum; and (d) X-ray diffraction (XRD) pattern of the nGO nanodrug carriers.

DOI: 10.1021/acsomega.7b02022
ACS Omega 2018, 3, 2396−2405

AFM measurements were conducted. Sonication treatment was effective to disperse nGO nanosheets with the thickness of about 1.2 and 50−250 nm in lateral width, indicating two- or three-layer sheets (Figure 2a,b), facilitating their entrance into the cells.[18,26]

Raman spectroscopy is a nondestructive characterization method to discover the ordered graphic or disordered crystal structures of carbon. As shown in Figure 2c, the G band of Raman spectrum of nGO was broadened and shifted upward to 1590 cm^{-1} due to stress. Concurrently, the intensity of the D band at 1360 cm^{-1} increased substantially, indicating the size decrease of the in-plane sp^2 domains because of the ultrasonic exfoliation and strong oxidation. The XRD pattern of nGO is also shown in Figure 2d. The (002) peak can be observed at 10.2° of the 2θ value, indicating that the interlayer distances of the nGO was about 1.05 nm.[47]

In this drug delivery system, PEG-modified nGO was used as a drug carrier with the aim to enhance biocompatibility. FA was used as targeting moieties and PTX was chosen as a model drug. The preparation process of the nanosized pGO-FA/PTX complex is shown in Scheme 1.

The FT-IR spectra of nGO, nGO-COOH, PEG-NH_2, and pGO are shown in Figure 3a, wherein the peaks at 1622 and 1730 cm^{-1} were ascribed to the main structure of graphene of C−C═C and C═O stretching vibrations, respectively. After coating with 4-br-PEG-NH_2, the weakening of epoxy groups (C−O−C) at 1050 cm^{-1} and carboxylic group (C═O) bands

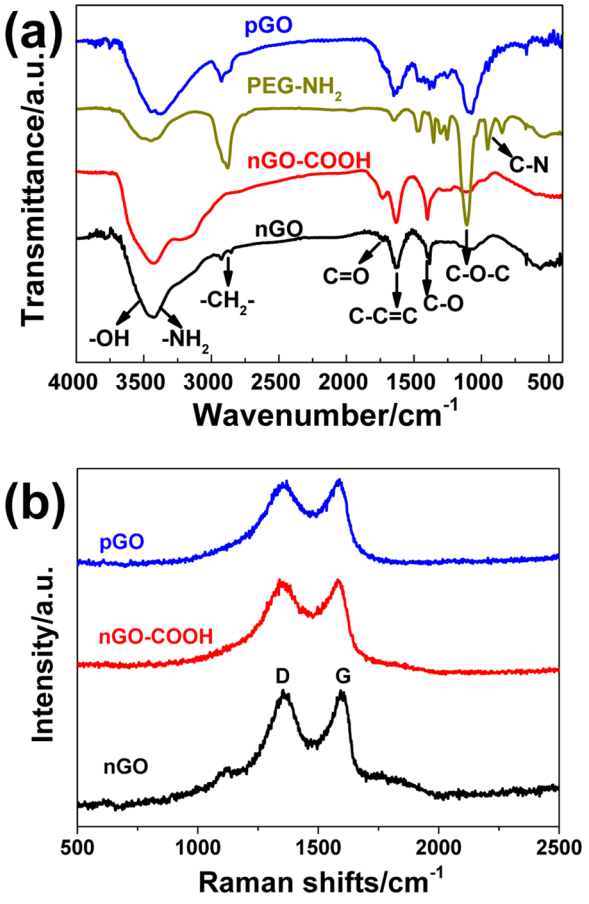

Figure 3. Modification of nGO with chloroacetic acid and PEG-NH_2: (a) FT-IR spectra of nGO samples modified with chloroacetic acid and PEG-NH_2 and (b) the Raman spectra of the modified nGO samples.

at 1730 cm^{-1} clearly indicated successful chemical grafting.[15] Furthermore, three new characteristic peaks at 1643 cm^{-1} (−CONH amide band I), 1569 cm^{-1} (−NH amide band II), and 1005 cm^{-1} (C−N stretching vibration) appeared, confirming the binding of 4-br-PEG-NH_2 chains onto the nGO surface. Meanwhile, another two strong peaks at 2870 cm^{-1} (−CH_2−) and 1405 cm^{-1} (−C−O−) also definitely illustrated the existence of PEG chains on the surface of nGO sheets, which can contribute to the enhancement of biocompatibility. As shown in Figure 3b and Table 1, the Raman spectra and intensity ratio (I_D/I_G) of the modified nGO exhibited similar results, indicating there was little change in the defects and edges during the modification processes.

As shown in Figure 4a, after functionalized by FA, the new characteristic peaks at 1000−1600 cm^{-1} appeared on pGO-FA, indicating the existence of benzene groups, suggesting that FA connected onto pGO surface. To further confirm the modification, the UV absorbance spectra of pGO before and after loading FA and PTX were recorded. As shown in Figure 4b, the UV absorbance spectrum of pGO showed a sharp absorption peak at 225 nm in the range of 200−400 nm. However, the sharp absorption peaks moved to a higher wavelength in the UV absorbance spectrum of pGO-FA, indicating the successful binding of FA. After mixing with PTX, the spectrum showed that sharp absorption peaks at 226, 254, and 336 nm originated from PTX with a characteristic peak at 229 nm, further verifying the successful loading of PTX to pGO-FA.

This phenomenon was also observed in the absorbance of the pGO and the decorated pGO suspension prepared in phosphate-buffered saline (PBS) after 24 h. The samples of pGO were suspended homogeneously in PBS, with an absorption peak at 230 nm, indicating that PEG-NH_2 increased the solubility of nanocarriers in PBS.[15]

As we know, many anticancer drugs such as PTX are aromatic and hydrophobic. Owing to their poor water solubility, the clinical applications are obviously limited. Herein, we chose PTX as a model drug to form pGO-FA-PTX nanocomplex for increasing the utilization rate of PTX.

The loading of PTX on pGO-FA was achieved by directly mixing PTX (dissolved in dimethyl sulfoxide (DMSO)) with pGO-FA aqueous suspension. The unbound or undissolved PTX was removed by centrifugation and filtration. The successful loading of PTX on pGO-FA was evidenced by the newly appeared characteristic absorption peak at 229 nm (originating from PTX) in the UV−vis absorbance spectrum (Figure 4b). As previously stated, drug cannot be loaded on PEG in a solution free of nGO; therefore, PTX loading was all attributed to the incorporation of nGO. However, there is a little amount of PTX decorated by covalent linking. Due to the lack of chemical reaction between PTX and pGO, physical adsorption of PTX could preserve its biological activity in comparison with the drug loading on the carrier via a covalent bond.

To further characterize the thickness, the average size, and the size distribution of the functional pGO sheets and drug-decorated samples, AFM characterization was conducted.[18] The AFM images, shown in Figure 5a, revealed that pGO presented a small increase in thickness from 1.2 to 1.6 nm. The 2D GO sheets with 40−200 nm of lateral dimension were a little smaller than nGO. These changes, compared to the interlayer spacing (1.2 nm) and size distribution of 50−250 nm in the

DOI: 10.1021/acsomega.7b02022
ACS Omega 2018, 3, 2396−2405

Table 1. Raman Intensity Ratios of nGO, nGO-COOH, and pGO

	G		D		
samples	shift (cm^{-1})	I_G (G-band intensity)	shift (cm^{-1})	I_D (D-band intensity)	I_D/I_G
nGO	1593	956	1354	963	1.0
nGO-COOH	1581	614	1339	615	1.0
pGO	1589	607	1351	588	0.97

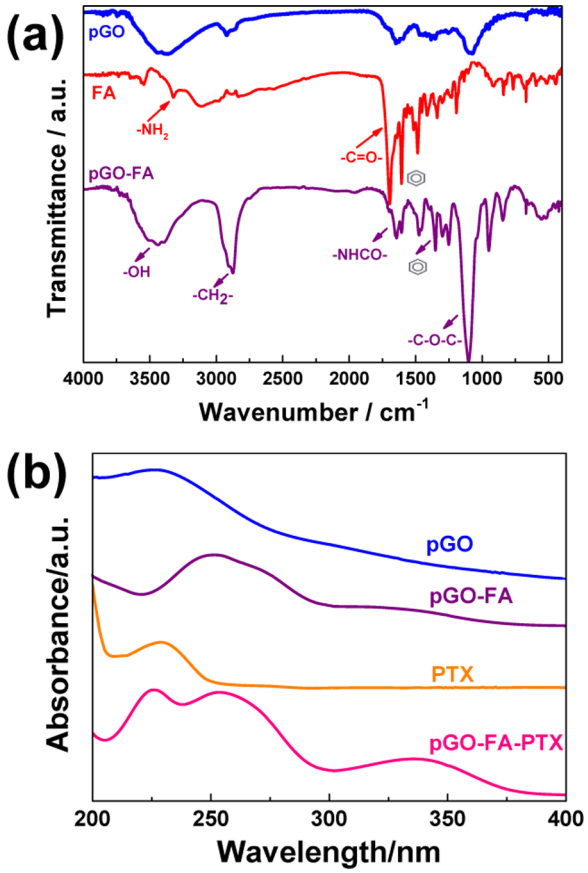

Figure 4. Structure characterization of the nanodrug systems decorated with FA and PTX: (a) FT-IR spectra of pGO before and after loading with FA and (b) the UV−vis absorbance spectra of pGO before and after loading with FA and PTX.

parent GO, were caused by the decoration of 4-br-PEG-NH_2 and the ultrasonication during the process.[48]

After being decorated by the target molecule, FA, as shown in Figure 5b, the pGO sheets were of ∼2.5 nm thickness and their lateral dimension was decreased, which may be caused by the modification and ultrasonication process. The pGO sheets were covered with FA on the both sides, indicating that FA had an average decorating thickness of ∼1.0 nm. After loading with PTX (Figure 5c), the thickness of the layer and roughness on the layer were further increased. The relatively high density of peaks shown in the 3D morphology photos clearly indicated the high loading capacity of PTX.

Cell Cytotoxicity. To investigate the cell cytotoxicity, blank carriers were examined firstly. pGO and pGO-FA were directly incubated with A2780 cells for 48 h in a 37 °C incubator. Then, a CCK-8 assay was used to examine the viability of A2780 cells. The result showed no significant decrease in cell viability (Figure 6), indicating that our as-synthesized nanocarrier had low cytotoxicity and good biocompatibility.

As shown in Figure 7, PTX had a dose-dependent (0−200 nM) cell inhibition effect on A2780 cells. Cell viability was kept high at 60% when treated with 200 nM of free PTX. However, pGO-FA-PTX with the same dose of PTX exhibited more significant cytotoxicity (cell viability less than 30%, 2 times lower than that of free PTX) toward A2780 cells than free PTX. That should be attributed to the nanocarriers, pGO-FA, with good biocompatibility, appropriate size, and target recognition, all of which made it more effective to deliver a number of drugs to perform a noticeable therapeutic effect.

Cellular cytotoxicity of anticancer drugs was then evaluated by fluorescence microscopy after incubation of A2780 cells with different concentrations of free drugs, or nanocomplexes. Then, the nuclei of A2780 cells were stained by 4′,6-diamidino-2-phenylindole (DAPI).[34] We can clearly observe the blue fluorescence in the cells after incubating for 24 h (Figure 8). As the drug concentration increases, the fluorescence intensity gradually decreases, indicating that the number of living cells was decreased slowly and the drugs or nanohybrids could be introduced into A2780 cells.

Compared with the free PTX-treated groups, the weaker fluorescence signal of DAPI was observed in the pGO-FA-PTX groups with the same PTX equivalent concentrations, illustrating that pGO-FA as a carrier could enter the cells and locate in the nuclei with high efficiency due to the special affinity interaction between FA and FA receptor overexpression in cancer cells. This experiment strongly suggests specific cytotoxicity of pGO-FA-PTX by A2780 cells, and that pGO-FA-PTX nanosystems can effectively deliver drugs to the target tumor cells.

As shown in Figure 9, the large π-conjugated structure of nGO can form a $\pi-\pi$ stacking interaction with these aromatic drugs and the two planes of nGO can both adsorb aromatic compounds, suggesting their potential application as drug carriers. Also, because there are many active amine groups on pGO, PTX can react with the groups on pGO and induce covalent immobilization. Moreover, recent reports declared that 2D shape and ultrasmall size of PEGylated graphene sheets had promising drug delivery properties, not only the highly efficient passive tumor targeting performance but also the relatively low retention in reticuloendothelial systems.

CONCLUSIONS

In this work, we reported the synthesis of the nanocarrier with good biocompatibility and good delivering performance of a water-insoluble anticancer drug of PTX. pGO and pGO-FA nanocarriers were proved to be nontoxic even at concentrations as high as 300 μg/mL practically, and the pGO-FA-PTX nanocomplex was found to be highly cytotoxicity to human ovarian cancer cell line A2780 in vitro as evaluated by WST-8 assay. The pGO-FA-PTX inhibited A2780 cells in a concentration- and time-dependent manner and had a 2 times higher cytotoxicity effect compared to free PTX, especially at lower concentration and shorter time, for improving the bioavailability of PTX. Furthermore, fluores-

DOI: 10.1021/acsomega.7b02022
ACS Omega 2018, 3, 2396−2405

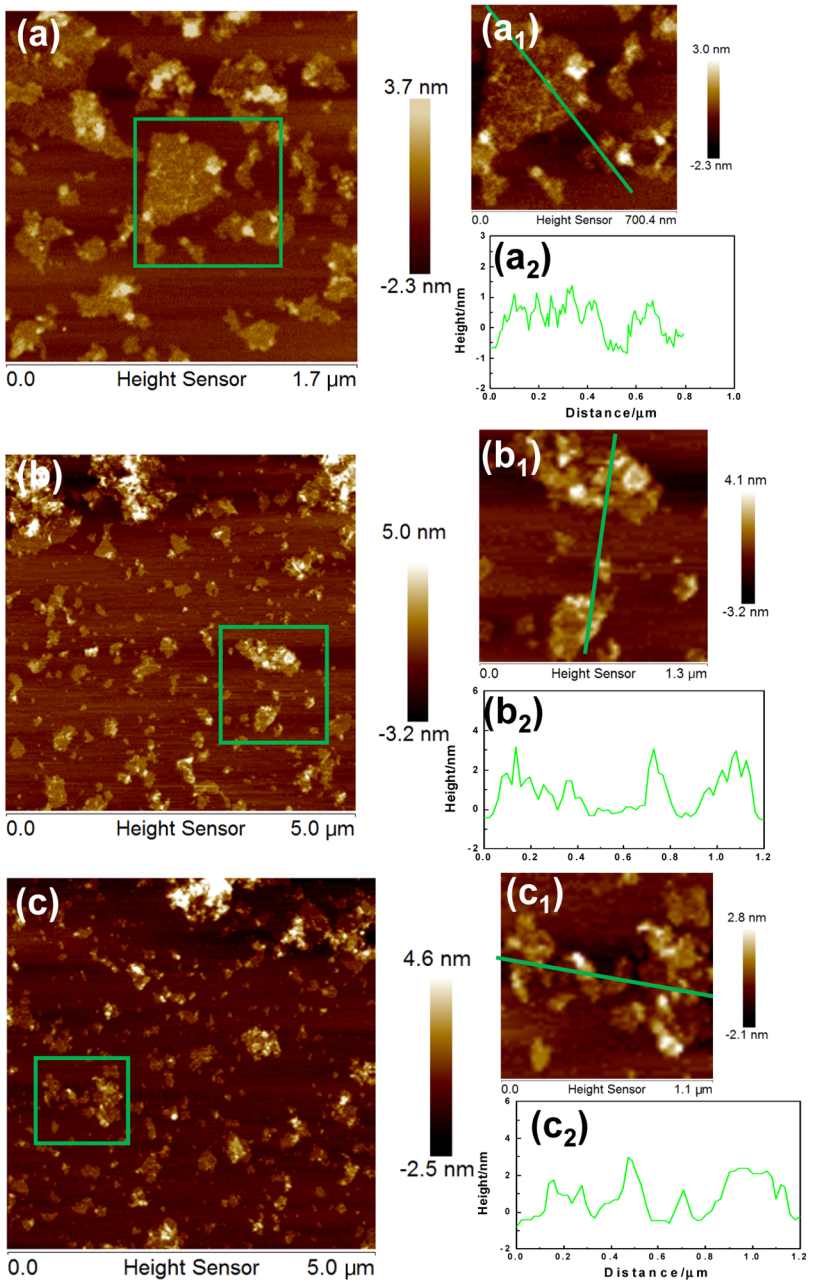

Figure 5. AFM images of the modified nanodrug carriers of nGO. (a, a_1) AFM image of pGO (nGO modified with 4-br-PEG-NH_2), (a_2) height profiles of line scannings in (a_1); (b, b_1) AFM image of pGO modified by FA and (b_2) height profiles of line scannings in (b_1); and (c, c_1) AFM image of pGO-FA loaded with PTX and (c_2) height profiles of line scannings in (c_1).

cence observation demonstrated that pGO-FA-PTX killed A2780 cells more effectively. The special affinity interaction between FA and FA receptor exhibited the overexpression in cancer cells. The prepared multifunctional pGO-FA-PTX would be a promising tumor theranostic agent for clinical application.

EXPERIMENTAL SECTION

Materials. The 4-arm PEG-NH_2 (99%) was purchased from SINOPEG Biotech Co., Ltd. (Xiamen, China). Folic acid (FA, 99%), paclitaxel (PTX, 99%), *N*-(3-dimethylaminopropyl-*N*′-ethylcarbodiimide) hydrochloride (EDC, 99%), 2-(*N*-morpholino) ethane sulfonic acid (99%), and hydroxy-2, 5-dioxopyrrolidine-3-sulfonic acid sodium salt (NHS, 99%) were purchased from Aladdin Reagent (Shanghai, China). The human ovarian cancer cell line A2780 was provided by Jiangsu Innovation Center for Industrial Biotechnology. All of the other chemicals were of analytical grade and directly used without further purification.

Synthesis of nGO and pGO. The sample of nGO was prepared with natural graphite powder following a modified Hummer's method.[42,43] To attach the PEG-NH_2, carboxylic acid functional groups were induced, as reported by our group before.[20]

Preparation of pGO-FA Nanohybrids. The targeting drug delivery system, pGO-FA, was developed by coupling of FA and pGO with an amide bond.[34] Briefly, EDC (192 mg) and NHS (54.25 mg) were added slowly to the pGO suspension as described in ref 14. Then, FA (146.6 mg) was added to the dispersion and the reaction was incubated

DOI: 10.1021/acsomega.7b02022
ACS Omega 2018, 3, 2396−2405

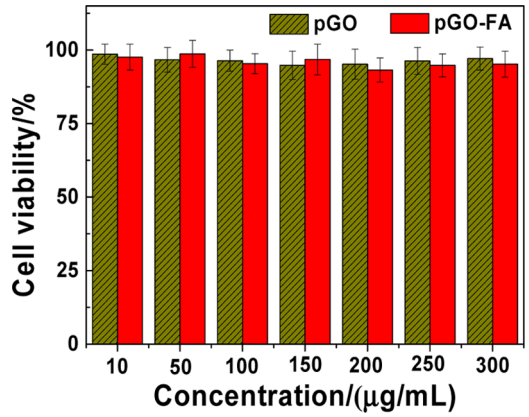

Figure 6. Cytotoxicity of different concentrations of pGO and pGO-FA on A2780 cells at 48 h treatment time. Error bars were based on triplet samples.

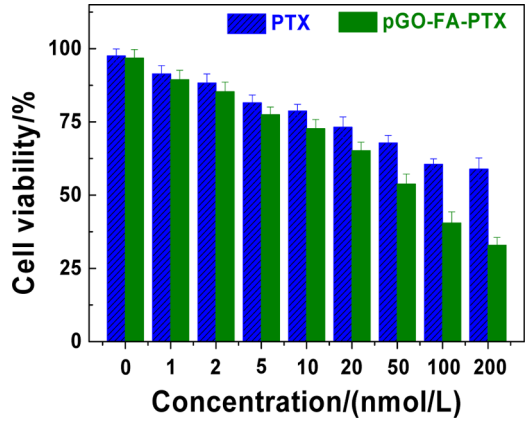

Figure 7. Cytotoxicity of different concentrations of free PTX and pGO-FA-PTX (at the same concentration of PTX) on A2780 cells (error bars are based on triplet samples).

overnight, yielding a pGO-FA solution, followed by filtration and water washing.

Loading of PTX on pGO-FA. To load PTX onto the pGO-FA sheets, PTX needed to be modified by succinic anhydride according to the literature.[14,44] First, PTX was modified by adding a carboxyl acid group on the molecule. The loading efficiency of PTX on the carrier of pGO was approximately 18.7%, obtained from UV−vis spectroscopy. Then, the modified PTX (contain 12.5 mg of PTX dissolved in pyridine 200 μL) was introduced to pGO-FA by amidation and physical absorption in the presence of EDC and NHS as described in Synthesis of nGO and pGO.

Cells Culture. Human ovarian cancer cell line A2780 was bought and cultured in RPMI 1640 medium supplemented with 10% fetal bovine serum at 37 °C under a 5% CO_2 and relative humidity of 90% atmosphere. The cells were adherent to the culture medium.

Cell Viability Assay. Human ovarian cancer cell line A2780 was plated in 96-well plates at a density of 5×10^3 cells per well in 100 μL of culture medium and added with different concentrations of pGO-FA, pGO-FA-PTX, and free PTX (dissolved in DMSO and diluted in PBS). The relative cell viability was measured by WST assay using CCK-8 kit. After treatment for 48 h, the absorbance of each well was measured at the wavelength of 450 nm, using a Tecan GENios Pro microplate reader.

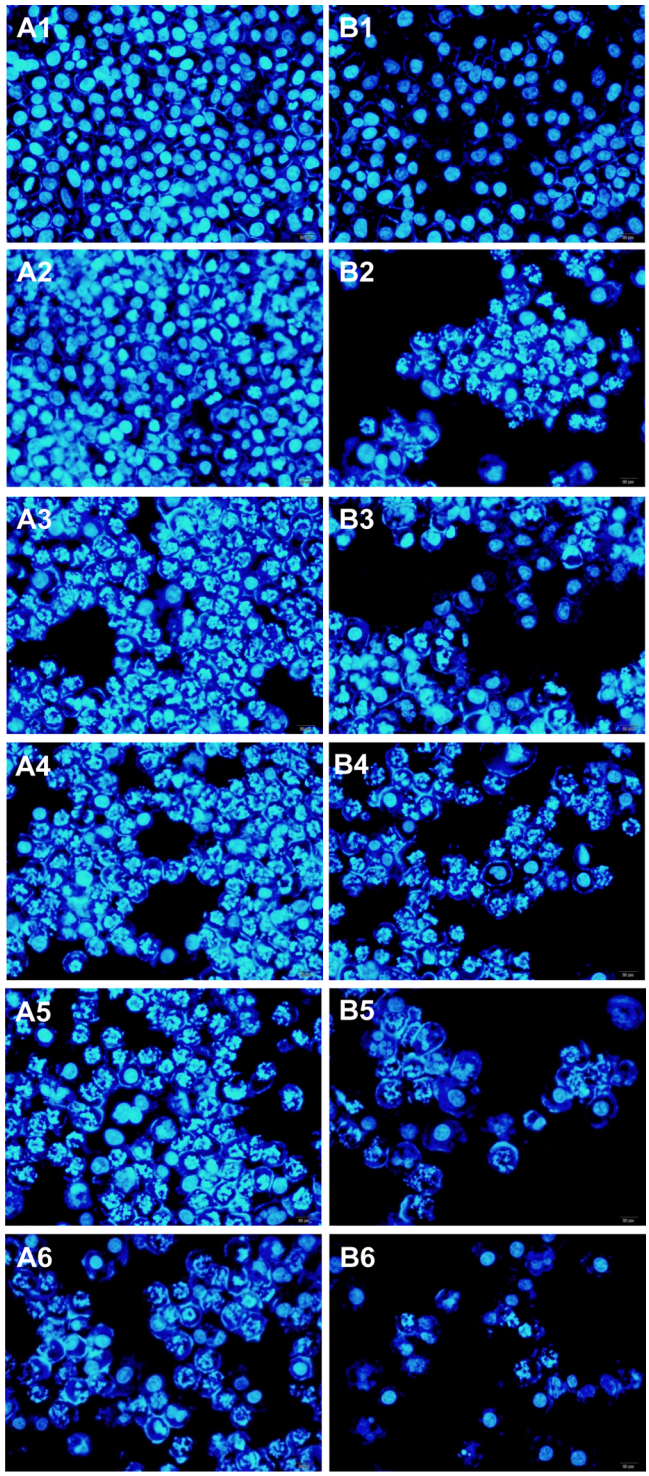

Figure 8. Fluorescent microscopy images showing the cell cytotoxicity of free PTX (A1: control; A2: 1 nmol/L; A3: 5 nmol/L; A4: 10 nmol/L; A5: 50 nmol/L; A6: 100 nmol/L) and pGO-FA-PTX (B1: control; B2: 1 nmol/L; B3: 5 nmol/L; B4: 10 nmol/L; B5: 50 nmol/L; B6: 100 nmol/L) by A2780 cells (at the same concentration of PTX) for 24 h.

DAPI Staining Analysis. A2780 cells were cultured with same concentrations of free PTX and pGO-FA-PTX for 2−200 nmol/L as described in ref 14, then fixed in 4% paraformaldehyde at 4 °C for 30 min, and stained with 4′,6-diamidino-2-phenylindole (DAPI, 2 μg/mL), a DNA-specific

DOI: 10.1021/acsomega.7b02022
ACS Omega 2018, 3, 2396−2405

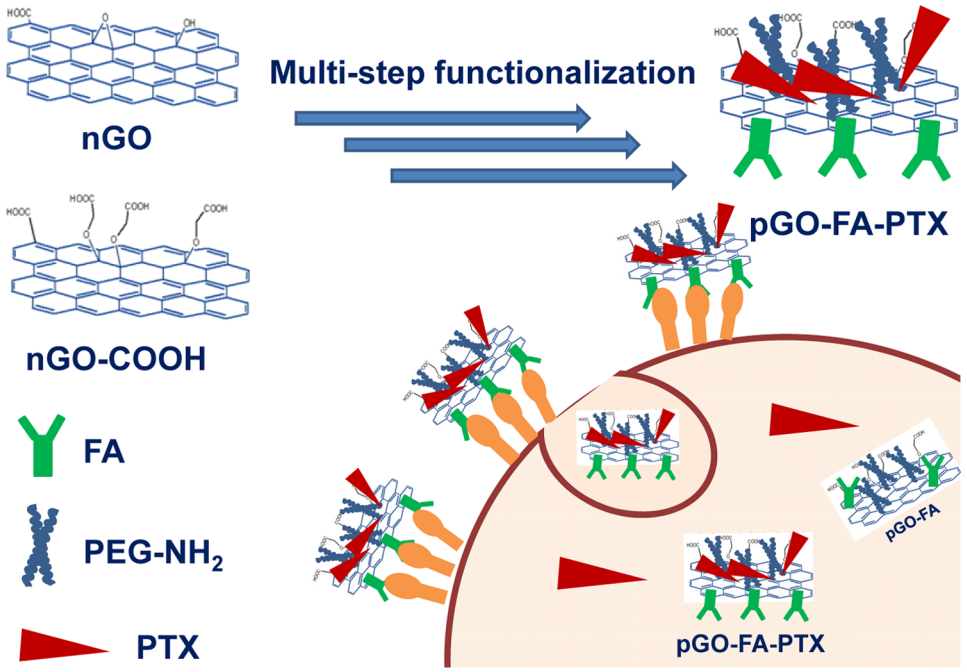

Figure 9. Schematic illustrate of pGO-FA-PTX as a functional drug delivery system for targeted therapy of human ovarian cancer cell line A2780.

fluorescent dye, at 37 °C for 10 min. The stained cells were imaged under a fluorescence microscope.

Characterization. The structure of the samples was characterized by Raman spectroscopy (Horiba Scientific, Irvine, CA), Fourier transform infrared (FT-IR, PerkinElmer, Spectrum BX II, Waltham, MA) spectroscopy, atomic force microscopy (AFM, CP-Research, Bruker, Billerica, MA), and powder X-ray diffraction (XRD, Bruker D8, Cu Kα radiation). Sample morphology and nanostructure were observed by field emission scanning electron microscopy (FESEM, Hitachi S-4800, Tokyo, Japan) and high-resolution transmission electron microscopy (HRTEM, Philips Tecnai G2 20 S-TWIN, Philips Innovation Services, Andover, MA), respectively. Ultraviolet and visible spectrophotometry (UV−vis, Evolution 260 Bio, Thermo) was used to observe the maximum absorption peak. Fluorescence spectrophotometry (F-7000, Hitachi) was applied to characterize cell cytotoxicity of the complexes.

AUTHOR INFORMATION

Corresponding Author

*E-mail: weizhuang@njtech.edu.cn. Phone/Fax: +86-25-5813-9389.

ORCID

Wei Zhuang: 0000-0002-1599-5405

Hanjie Ying: 0000-0002-4061-0001

Author Contributions

The paper was written through contributions of all of the authors. All of the authors have given approval to the final version of the manuscript.

Notes

The authors declare no competing financial interest.

ACKNOWLEDGMENTS

This work was supported by grants from the Program for Changjiang Scholars and Innovative Research Team in University (IRT_14R28), the Major Research Plan of the National Natural Science Foundation of China (21390204), the National Natural Science Foundation of China (Grant Nos. 21636003 and 21506090), the National Science Foundation of Jiangsu province (BK20141500), Open Fund by Jiangsu Key Lab of Biomass-based Green Fuels and Chemicals (No. JSBGFC14005), Jiangsu National Synergetic Innovation Center for Advanced Materials (SICAM), and the Priority Academic Program Development of Jiangsu Higher Education Institutions (PAPD).

REFERENCES

(1) Hubbell, J. A.; Chilkoti, A. Nanomaterials for Drug Delivery. *Science* **2012**, *337*, 303−305.

(2) Barretina, J.; Caponigro, G.; Stransky, N.; Venkatesan, K.; Margolin, A. A.; Kim, S.; Wilson, C. J.; Lehar, J.; Kryukov, G. V.; Sonkin, D.; Reddy, A.; Liu, M.; Murray, L.; Berger, M. F.; Monahan, J. E.; Morais, P.; Meltzer, J.; Korejwa, A.; Jane-Valbuena, J.; Mapa, F. A.; Thibault, J.; Bric-Furlong, E.; Raman, P.; Shipway, A.; Engels, I. H.; Cheng, J.; Yu, G. K.; Yu, J.; Aspesi, P.; de Silva, M.; Jagtap, K.; Jones, M. D.; Wang, L.; Hatton, C.; Palescandolo, E.; Gupta, S.; Mahan, S.; Sougnez, C.; Onofrio, R. C.; Liefeld, T.; MacConaill, L.; Winckler, W.; Reich, M.; Li, N.; Mesirov, J. P.; Gabriel, S. B.; Getz, G.; Ardlie, K.; Chan, V.; Myer, V. E.; Weber, B. L.; Porter, J.; Warmuth, M.; Finan, P.; Harris, J. L.; Meyerson, M.; Golub, T. R.; Morrissey, M. P.; Sellers, W. R.; Schlegel, R.; Garraway, L. A. The Cancer Cell Line Encyclopedia enables predictive modelling of anticancer drug sensitivity. *Nature* **2012**, *483*, 603−307.

(3) Singla, A. K.; Garg, A.; Aggarwal, D. Paclitaxel and Its Formulations. *Int. J. Pharm.* **2002**, *235*, 179−192.

(4) Siegel, R.; Naishadham, D.; Jemal, A. Cancer Statistics, 2013. *Ca-Cancer J. Clin.* **2013**, *63*, 11−30.

(5) Swain, A. K.; Pradhan, L.; Bahadur, D. Polymer Stabilized Fe3O4-Graphene as an Amphiphilic Drug Carrier for Thermo-Chemotherapy of Cancer. *ACS Appl. Mater. Interfaces* **2015**, *7*, 8013−8022.

(6) Mazrad, Z. A. I.; Choi, C. A.; Kim, S. H.; Lee, G.; Lee, S.; In, I.; Lee, K. D.; Park, S. Y. Target-specific induced hyaluronic acid decorated silica fluorescent nanoparticles@polyaniline for bio-imaging guided near-infrared photothermal therapy. *J. Mater. Chem. B* **2017**, *5*, 7099−7108.

DOI: 10.1021/acsomega.7b02022
ACS Omega 2018, 3, 2396−2405

(7) Pattni, B. S.; Chupin, V. V.; Torchilin, V. P. *Chem. Rev.* **2015**, *115*, 10938−10966.
(8) Wang, C.; Mallela, J.; Garapati, U. S.; Sowndharya Ravi, M.; Vignesh Chinnasamy, M.; Yvonne Girard, M.; Mark Howell, M.; Subhra Mohapatra, P. A chitosan-modified graphene nanogel for noninvasive controlled drug release. *Nanomedicine* **2013**, *9*, 903−911.
(9) Kazemzadeh-Narbat, M.; Lai, B. F. L.; Ding, C.; Kizhakkedathu, J. N.; Hancock, R. E. W.; Wang, R. Multilayered coating on titanium for controlled release of antimicrobial peptides for the prevention of implant-associated infections. *Biomaterials* **2013**, *34*, 5969−5977.
(10) Ma, N.; Liu, J.; He, W. X.; Li, Z. H.; Luan, Y. X.; Song, Y. M.; Garg, S. Folic acid-grafted bovine serum albumin decorated graphene oxide: An efficient drug carrier for targeted cancer therapy. *J. Colloid Interface Sci.* **2017**, *490*, 598−607.
(11) Tian, J.; Luo, Y.; Huang, L.; Feng, Y.; Ju, H.; Yu, B.-Y. Pegylated folate and peptide-decorated graphene oxide nanovehicle for in vivo targeted delivery of anticancer drugs and therapeutic self-monitoring. *Biosens. Bioelectron.* **2016**, *80*, 519−524.
(12) Wang, H.; Wang, K.; Mu, Q.; Stephen, Z. R.; Yu, Y.; Zhou, S.; Zhang, M. Mesoporous carbon nanoshells for high hydrophobic drug loading, multimodal optical imaging, controlled drug release, and synergistic therapy. *Nanoscale* **2017**, *9*, 1434−1442.
(13) Liao, J.; Wei, X. W.; Ran, B.; Peng, J. R.; Qu, Y.; Qian, Z. Y. Polymer hybrid magnetic nanocapsules encapsulating IR820 and PTX for external magnetic field-guided tumor targeting and multifunctional theranostics. *Nanoscale* **2017**, *9*, 2479−2491.
(14) Xu, Z.; Zhu, S. J.; Wang, M. W.; Li, Y. J.; Shi, P.; Huang, X. Y. Delivery of Paclitaxel Using PEGylated Graphene Oxide as a Nanocarrier. *ACS Appl. Mater. Interfaces* **2015**, *7*, 1355−1363.
(15) Xu, Z.; Wang, S.; Li, Y.; Wang, M.; Shi, P.; Huang, X. Covalent Functionalization of Graphene Oxide with Biocompatible Poly(ethylene glycol) for Delivery of Paclitaxel. *ACS Appl. Mater. Interfaces* **2014**, *6*, 17268−17276.
(16) Yin, T.; Liu, J. Y.; Zhao, Z. K.; Zhao, Y. Y.; Dong, L. H.; Yang, M.; Zhou, J. P.; Huo, M. R. Redox Sensitive Hyaluronic Acid-Decorated Graphene Oxide for Photothermally Controlled Tumor-Cytoplasm Selective Rapid Drug Delivery. *Adv. Funct. Mater.* **2017**, *27*, No. 1604620.
(17) Georgakilas, V.; Tiwari, J. N.; Kemp, K. C.; Perman, J. A.; Bourlinos, A. B.; Kim, K. S.; Zboril, R. Noncovalent Functionalization of Graphene and Graphene Oxide for Energy Materials, Biosensing, Catalytic, and Biomedical Applications. *Chem. Rev.* **2016**, *116*, 5464−5519.
(18) Sun, X.; Liu, Z.; Welsher, K.; Robinson, J. T.; Goodwin, A.; Zaric, S.; Dai, H. J. Nano-Graphene Oxide for Cellular Imaging and Drug Delivery. *Nano Res.* **2008**, *1*, 203−212.
(19) Feng, L.; Liu, Z. A. Graphene in biomedicine: opportunities and challenges. *Nanomedicine* **2011**, *6*, 317−324.
(20) Liu, Z.; Robinson, J. T.; Sun, X.; Dai, H. PEGylated Nanographene Oxide for Delivery of Water-Insoluble Cancer Drugs. *J. Am. Chem. Soc.* **2008**, *130*, 10876−10877.
(21) Miao, W.; Shim, G.; Lee, S.; Lee, S.; Choe, Y. S.; Oh, Y.-K. Safety and tumor tissue accumulation of pegylated graphene oxide nanosheets for co-delivery of anticancer drug and photosensitizer. *Biomaterials* **2013**, *34*, 3402−3410.
(22) Gao, P.; Liu, M. Y.; Tian, J. W.; Deng, F. J.; Wang, K.; Xu, D. Z.; Liu, L. J.; Zhang, X. Y.; Wei, Y. Improving the drug delivery characteristics of graphene oxide based polymer nanocomposites through the "one-pot" synthetic approach of single-electron-transfer living radical polymerization. *Appl. Surf. Sci.* **2016**, *378*, 22−29.
(23) Zheng, X. T.; Ma, X. Q.; Li, C. M. Highly efficient nuclear delivery of anti-cancer drugs using a bio-functionalized reduced graphene oxide. *J. Colloid Interface Sci.* **2016**, *467*, 35−42.
(24) Karimi, M.; Ghasemi, A.; Zangabad, P. S.; Rahighi, R.; Basri, S. M. M.; Mirshekari, H.; Amiri, M.; Pishabad, Z. S.; Aslani, A.; Bozorgomid, M.; Ghosh, D.; Beyzavi, A.; Vaseghi, A.; Aref, A. R.; Haghani, L.; Bahrami, S.; Hamblin, M. R. Smart micro/nanoparticles in stimulus-responsive drug/gene delivery systems. *Chem. Soc. Rev.* **2016**, *45*, 1457−1501.
(25) Zhang, S.; Xiong, P.; Yang, X.; Wang, X. Novel PEG Functionalized Graphene Nanosheets: Enhancement of Dispersibility and Thermal Stability. *Nanoscale* **2011**, *3*, 2169−2174.
(26) HaiQing, D.; ZhiLei, Z.; HuiYun, W.; YongYong, L.; FangFang, G.; AiJun, S.; Frank, P.; Chao, L.; DongLu, S. Poly(ethylene glycol) Conjugated Nano-Graphene Oxide for Photodynamic Therapy. *Sci. China Chem.* **2010**, *53*, 2265−2271.
(27) Shi, Y. G.; Liu, M. Y.; Wang, K.; Huang, H. Y.; Wan, Q.; Tao, L.; Fu, L. H.; Zhang, X. Y.; Wei, Y. Direct surface PEGylation of nanodiamond via RAFT polymerization. *Appl. Surf. Sci.* **2015**, *357*, 2147−2153.
(28) Heng, C. N.; Zheng, X. Y.; Liu, M. Y.; Xu, D. Z.; Huang, H. Y.; Deng, F. J.; Hui, J. F.; Zhang, X. Y.; Wei, Y. Fabrication of luminescent hydroxyapatite nanorods through surface-initiated RAFT polymerization: Characterization, biological imaging and drug delivery applications. *Appl. Surf. Sci.* **2016**, *386*, 269−275.
(29) Wu, M.; Guo, X.; Zhao, F.; Zeng, B. A Poly(ethylenglycol) Functionalized ZIF-8 Membrane Prepared by Coordination-Based Post-Synthetic Strategy for the Enhanced Adsorption of Phenolic Endocrine Disruptors from Water. *Sci. Rep.* **2017**, *7*, No. 8912.
(30) Yang, K.; Hu, L. L.; Ma, X. X.; Ye, S. Q.; Cheng, L.; Shi, X. Z.; Li, C. H.; Li, Y. G.; Liu, Z. Multimodal Imaging Guided Photothermal Therapy using Functionalized Graphene Nanosheets Anchored with Magnetic Nanoparticles. *Adv. Mater.* **2012**, *24*, 1868−1872.
(31) Chang, Y.; Yang, S. T.; Liu, J. H.; Dong, E.; Wang, Y. W.; Cao, A. N.; Liu, Y. F.; Wang, H. F. In vitro toxicity evaluation of graphene oxide on A549 cells. *Toxicol. Lett.* **2011**, *200*, 201−210.
(32) He, S. J.; Song, B.; Li, D.; Zhu, C. F.; Qi, W. P.; Wen, Y. Q.; Wang, L. H.; Song, S. P.; Fang, H. P.; Fan, C. H. A Graphene Nanoprobe for Rapid, Sensitive, and Multicolor Fluorescent DNA Analysis. *Adv. Funct. Mater.* **2010**, *20*, 453−459.
(33) Bai, H.; Li, C.; Wang, X. L.; Shi, G. Q. A pH-sensitive graphene oxide composite hydrogel. *Chem. Commun.* **2010**, *46*, 2376−2378.
(34) Huang, P.; Xu, C.; Lin, J.; Wang, C.; Wang, X.; Zhang, C.; Zhou, X.; Guo, S.; Cui, D. Folic Acid-conjugated Graphene Oxide loaded with Photosensitizers for Targeting Photodynamic Therapy. *Theranostics* **2011**, *1*, 240−250.
(35) Zhang, L.; Xia, J. G.; Zhao, Q. H.; Liu, L. W.; Zhang, Z. J. Functional Graphene Oxide as a Nanocarrier for Controlled Loading and Targeted Delivery of Mixed Anticancer Drugs. *Small* **2010**, *6*, 537−544.
(36) Chen, C.; Ke, J.; Zhou, X. E.; Yi, W.; Brunzelle, J. S.; Li, J.; Yong, E.-L.; Xu, H. E.; Melcher, K. Structural basis for molecular recognition of folic acid by folate receptors. *Nature* **2013**, *500*, 486−489.
(37) Ji, X.; Song, Y. H.; Han, J.; Ge, L.; Zhao, X. X.; Xu, C.; Wang, Y. Q.; Wu, D.; Qiu, H. X. Preparation of a stable aqueous suspension of reduced graphene oxide by a green method for applications in biomaterials. *J. Colloid Interface Sci.* **2017**, *497*, 317−324.
(38) Wang, K.; Fan, X. L.; Zhao, L. Y.; Zhang, X. Y.; Zhang, X. Q.; Li, Z.; Yuan, Q.; Zhang, Q. S.; Huang, Z. F.; Xie, W. S.; Zhang, Y. Y.; Wei, Y. Aggregation Induced Emission Fluorogens Based Nanotheranostics for Targeted and Imaging-Guided Chemo-Photothermal Combination Therapy. *Small* **2016**, *12*, 6568−6575.
(39) Cheng, K. W.; Lahad, J. P.; Kuo, W.-l.; Lapuk, A.; Yamada, K.; Auersperg, N.; Liu, J.; Smith-McCune, K.; Lu, K. H.; Fishman, D.; Gray, J. W.; Mills, G. B. The RAB25 small GTPase determines aggressiveness of ovarian and breast cancers. *Nat. Med.* **2004**, *10*, 1251.
(40) Hu, X.-W.; Meng, D.; Fang, J. Apigenin inhibited migration and invasion of human ovarian cancer A2780 cells through focal adhesion kinase. *Carcinogenesis* **2008**, *29*, 2369−2376.
(41) Yunos, N. M.; Beale, P.; Yu, J. Q.; Strain, D.; Huq, F. Studies on Combinations of Platinum with Paclitaxel and Colchicine in Ovarian Cancer Cell Lines. *Anticancer Res.* **2010**, *30*, 4025−4037.
(42) Hummers, W. S.; Offeman, R. E. Preparation of Graphitic Oxide. *J. Am. Chem. Soc.* **1958**, *80*, 1339.
(43) Chen, D.; Feng, H.; Li, J. Graphene Oxide: Preparation, Functionalization, and Electrochemical Applications. *Chem. Rev.* **2012**, *112*, 6027−6053.

DOI: 10.1021/acsomega.7b02022
ACS Omega 2018, 3, 2396−2405

(44) Arya, N.; Arora, A.; Vasu, K. S.; Sood, A. K.; Katti, D. S. Combination of single walled carbon nanotubes/graphene oxide with paclitaxel: a reactive oxygen species mediated synergism for treatment of lung cancer. *Nanoscale* **2013**, *5*, 2818−2829.
(45) Stankovich, S.; Dikin, D. A.; Piner, R. D.; Kohlhaas, K. A.; Kleinhammes, A.; Jia, Y.; Wu, Y.; Nguyen, S. T.; Ruoff, R. S. Synthesis of graphene-based nanosheets via chemical reduction of exfoliated graphite oxide. *Carbon* **2007**, *45*, 1558−1565.
(46) Tian, B.; Wang, C.; Zhang, S.; Feng, L. Z.; Liu, Z. Photothermally Enhanced Photodynamic Therapy Delivered by Nano-Graphene Oxide. *ACS Nano* **2011**, *5*, 7000−7009.
(47) Krishnamoorthy, K.; Veerapandian, M.; Yun, K.; Kim, S. J. The Chemical and structural analysis of graphene oxide with different degrees of oxidation. *Carbon* **2013**, *53*, 38−49.
(48) Li, D.; Müller, M. B.; Gilje, S.; Kaner, R. B.; Wallace, G. G. Processable aqueous dispersions of graphene nanosheets. *Nat. Nanotechnol.* **2008**, *3*, 101.

DOI: 10.1021/acsomega.7b02022
ACS Omega 2018, 3, 2396−2405